The Center for Particle Theory

THE UNIVERSITY OF TEXAS AT AUSTIN

What Can We Learn From High-Energy Hadron-Nucleus Interactions?*

CONF-800120--5

by

Don M. Tow

(Center for Particle Theory, Department of Physics
University of Texas, Austin, Texas 78712, USA)

Abstract

High-energy hadron-nucleus (hA) collisions provide the exciting possibility of giving information about the spacetime development of hadron-hadron interactions and therefore differentiating various multiparticle production models. We review some of the major developments in this field during the past decade, both experimentally and theoretically. Several general features of the data are pointed out, and several classes of models are discussed. We elaborate on a recently proposed simple spacetime model for high-energy hA collisions. We briefly comment on the extension to nucleus-nucleus interactions and the future outlook.

*To be published in the Proceedings of the 1980 Gaungzhou (Canton) Conference on Theoretical Particle Physics, January 5-11, 1980, Gaungzhou, People's Republic of China.

I. Introduction

In hadron-hadron (hh) scattering experiments, because the particle detectors are always at macroscopic distances from the interaction region,[1] one can never learn about the spacetime development of the strongly interacting process. In other words, hh scattering experiments can only measure the S-matrix. On the other hand, if one replaces the target hadron by a nuclear target, then the time of flight for the incident hadron or any produced secondary in traveling from the first nucleon to a succeeding nucleon in the nucleus is of the same order or even shorter than the typical duration of the strongly interacting process. This means the nucleons in the nucleus serve as detectors which are separated by microscopic distances. Therefore, hadron-nucleus (hA) scattering experiments offer the unique opportunity to learn about the spacetime development of a strongly interacting process. Furthermore, one of the most important areas of research in strong interaction during the past decade is to find the correct model for describing high-energy multiparticle production processes. Since different multiparticle production models for hh collisions give rise in general to different predictions for hA collisions, studying hA interactions provides a good possibility of discriminating among the various multiparticle production models and selecting the correct one. For these reasons, high-energy hA collisions have generated tremendous interest during the past few years, both experimentally and theoretically.

In this paper, we present a brief review of this subject.[2] In Section II we review the essential features of the experimental multiparticle production data. In Section III we discuss several types of hA models. Here we also elaborate on a recently proposed simple spacetime model for high-energy hA collisions. This is followed by a short section on the extension to nucleus-nucleus (AA) collisions. In the last section, we mention some other interesting effects arising from interactions with nuclear targets, and end with some conclusions and an outlook.

II. Experimental Features

There are several general features of the data.[3] One defines

$$\bar{\nu}_h \equiv \frac{A\sigma_{in}^{hN}}{\sigma_{in}^{hA}} , \qquad \text{(II.1)}$$

where σ_{in}^{hN} (σ_{in}^{hA}) is the hadron-nucleon (nucleus) inelastic cross section and A is the number of nucleons in the nucleus. The variable $\bar{\nu}_h$ can be interpreted to be the average number of inelastic collisions experienced by the hadron h as it traverses the nucleus (see Appendix A). Experimentally $\bar{\nu}_h$ is approximately energy independent in the Fermilab energy range. Table I gives the values of $\bar{\nu}$ for p and $\pi^{\pm}$ from an experiment[3b] in the energy range from 50 GeV to 200 GeV.

Table I

Element	A	$\bar{\nu}_p$	$\bar{\nu}_\pi$
H	1	1.00	1.00
C	12	1.52	1.39
Al	27	1.95	1.70
emulsion	~60	2.50	2.07
Cu	64	2.54	2.10
Ag	108	3.00	2.40
Pb	207	3.67	2.82
U	238	3.84	2.92

If one defines

$$R_A \equiv \frac{\langle N_{ch}\rangle_{hA}}{\langle N_{ch}\rangle_{hN}} , \qquad \text{(II.2)}$$

then the first feature is

(a) R_A is small (~2.5) even for the largest A (see Fig. 1) and may be approximately parametrized as

$$R_A \simeq a + b\bar{\nu} , \quad \text{with } a \simeq 1/2 \simeq b , \qquad \text{(II.3)}$$

where a and b are roughly energy independent in the Fermilab range.[4]

Let η and y be the pseudorapidity and rapidity variable, respectively, defined as $\eta \equiv -\ln \tan(\theta_L/2)$ and $y = \frac{1}{2}\ln \frac{E + P_z}{E - P_z}$, where θ_L is the laboratory scattering angle, E and P_z are the energy and longitudinal momentum of the particle. Experimentally it is easier to measure η, whereas theoretically it is more convenient to use y. For almost all practical purposes, they can be used interchangeably. In any case one can always change from one to another by a simple kinematical transformation. The second feature is

(b) the differential multiplicity distribution $dN/d\eta$ is approximately target independent in the projectile fragmentation region and increases roughly as $\bar{\nu}_h$ in the target fragmentation region, as shown in Fig. 2.

Different projectiles give rise to different $\bar{\nu}_h$ and result in different R_A and $dN/d\eta$ for the same A. However, if we choose A such that we have the same $\bar{\nu}$ for different projectiles, then the third feature is

(c) different projectiles but for the same $\bar{\nu}$ have almost the same R_A[3f,3h] and $dN/d\eta$.[3b]

As usual, one defines the elasticity to be the ratio of the laboratory energy of the outgoing projectile to the incident projectile's laboratory energy. For proton or neutron initiated reactions, there is little ambiguity in picking among the final hadrons the one corresponding to the projectile nucleon, because usually there is only one nucleon in the forward hemisphere. The fourth experimental feature is

(d) The elasticity for hA collisions decreases only slightly from that of hN collisions even for the largest A.[5]

Another feature is

(e) in the very forward region, i.e., for $\eta \sim \eta_{max}$, $\left(\frac{dN}{d\eta}\right)^{hA_2} < \left(\frac{dN}{d\eta}\right)^{hA_1}$ by a small amount for $A_2 > A_1$.[3e]

Finally, if one defines

$$D \equiv \sqrt{\langle N_{ch}^2 \rangle - \langle N_{ch} \rangle^2} \quad , \qquad \text{(II.3)}$$

(f) then one sees a linear dependence of the dispersion D on $\langle N_{ch} \rangle$, and the data points for various nuclei lie on the same straight line.[3a]

The above are six general features of the high-energy hA data. A successful model must explain most and eventually all of these features.

III. Theoretical Models

We discuss several types of theoretical models for high-energy hA collisions.

A. Naive Cascade Model

The most obvious model and one of the earliest models proposed is the "naive cascade model."[6] This model assumes that in hh collision, the time involved in producing physical or fully dressed secondaries[7] is very short. Therefore, in hA collision, the incident hadron h interacts with one of the nucleons near the surface of A and produces many hadrons; each of these hadrons then undergoes further interactions with the subsequent nucleons, and the process repeats until all the hadrons emerge from A. This model results in an extremely large multiplicity and is completely ruled out by the experimental result (II.3). The smallness of R_A means that for a model to have any chance of explaining the data, it must have a mechanism to freeze some of the degrees of freedom.

B. Coherent Tube Model

A high-energy incident hadron h sees the nucleus Lorentz-contracted, a second type of model[8] assumes that h interacts coherently with a tube of $\bar{\nu}_h$ nucleons. In this "coherent tube model," the net effect is that the target has a mass $\bar{\nu}_h m_N$ and gives rise to an effective incident energy of $\bar{\nu}_h E_{inc}$. This model results in an enlargement along the negative direction of the target fragmentation region. Since at present energies the inclusive distribution has not reached a plateau and its height is increasing with energy, the model does give rise to an increase in the height of $\frac{dN}{d\eta}$ for hA collisions. However, this increase is much too small to be compatible with the data.[3b,d] Therefore, we conclude that it is unlikely that the coherent tube mechanism is the dominant mechanism responsible for the bulk of the multiparticle events in hA collisions. But this does not rule out the existence of this mechanism. As a matter of fact, it is probable that it is the coherent tube mechanism which is responsible for those rare and interesting events associated with the cumulative effect.[9] Better data and perhaps also particle identification in the region $\eta \lesssim 0$ can shed light on the existence and significance of the coherent tube mechanism.

C. Long-Interaction-Time Model

From phenomenological analysis of multiparticle production in hh interaction, one concludes that a general property of hh interaction is short-range correlation in rapidity space. One of the consequences of this property is that for the incident hadron to interact with the target nucleon, it must generate a multiperipheral chain containing small rapidity particles (or partons). The rapidity difference between the latter and the target (or partons in the target) is then small and appreciable interaction can occur. Now, it takes time for a hadron to generate such a multiperipheral chain. Focusing on one link in this multiperipheral chain, one can argue from the uncertainty relation and the difference between the initial energy and the final energy that the time τ_0 (in the rest frame of the parent hadron) for the hadron to branch into two hadrons is of the order $\tau_0 \sim 1/m$, where m is the mass of the hadrons. In the laboratory frame this time is Lorentz dilated. Summing the times from all the links results in a total laboratory time given approximately by $\tau \sim \frac{E}{m} \tau_0$, where E is the energy of the incident hadron. Therefore, at high energies a long interaction time is involved. For hA collisions, h can begin to generate its multiperipheral chain while approaching A. However, for the energetic secondaries produced from the interaction of h with one of the nucleons in A, they will not be able to interact with the subsequent nucleons, because by the time they generate these small rapidity multiperipheral chains, they would have travelled a long distance and be spatially separated from A (see Fig. 3). Therefore, only the small momentum secondaries can cascade and the additional multiplicity must be concentrated in the small rapidity region, and such long-interaction-time model[10] is at least in qualitative agreement with the data. Several of these models have also been shown to be in quantitative agreement.[10f-10i] But some of these require additional assumptions. Davidenko and Nikolaev[10f] used a $\tau_0 \sim \frac{1}{150m_\pi}$ which is much smaller than the τ_0 discussed earlier (this possibility was also discussed in Ref. [10h]). Capella and Kryzwicki[10g] suppressed all secondary cascades and assumed that several constituents of the projectile, each of which shares the incident energy roughly equally, interact with the corresponding number of nucleons in A. Bialkowski, Chiu, and Tow[10h] assumed that the probability for a produced secondary to develop a small momentum multiperipheral chain is enhanced in the presence of other hadronic matter, as in a nucleus (induced maturity concept). Valanju, Sudarshan, and Chiu[10i] generalized Feinberg's QED result[10a] and thus provided a theoretical justification for the immaturity concept of Ref. [10h]. Furthermore, by using a continuous hadronic medium for the nucleus, instead of the discrete one used in Ref. [10h], they derived naturally a factor which at present energies has the same numerical effect as the induced maturity factor used in Ref. [10h]. Therefore, to explain present hA data, it is not necessary to explicitly introduce the induced maturity concept.

Thus, this type of long-interaction-time model, perhaps with some additional assumption, has been shown to be able to explain the experimental data. This type of model has also been extended to photon- and lepton-nucleus collisions.[11]

D. Two-Sheeted Model

The previous type of model assumes that the secondary particles are produced almost instantaneously, but in some sense they are bare particles, because they have a smaller inelastic collision probability than ordinary physical particles. To dress up these particles involves a long time (the larger the momentum, the longer the time).

Another type of model[12] takes an alternative approach to freeze some of the degrees of freedom. It assumes that in hh collisions, the result of the interaction is two excited hadronic systems. Each hadronic system is consisted of a color-$\overline{3}$ diquark and a color-3 quark; in the CM system the diquark has large momentum and the quark has small momentum. Because of the large momentum difference, the spatial separation between the diquark and the quark increases with time, and the colored confining mechanism then presumably comes into play and causes each hadronic system to evolve into a jet of hadrons after a characteristic time τ_0 (in its own rest frame) has elapsed (see Fig. 4). For incident energy in the Fermilab range, the invariant mass of each hadronic system is several GeV's; so it is reasonable to take τ_0 to be the typical lifetime of a heavy nucleon resonance, i.e., $\tau_0 \approx 1/m_\pi$ or $1/2m_\pi$. Then at high energy, the lifetime of the excited projectile system (EPS) in the laboratory will be greatly Lorentz dilated, whereas the lifetime of the excited target system (ETS) will have a small Lorentz dilation factor. Therefore, in high energy hA collision, the first EPS does not have time to evolve into its final multi-hadron state before it reaches the next nucleon in A, whereas the ETS will have a large probability of evolving into its final multihadron state. The above process repeats itself until the EPS leaves A after $\bar{\nu}_h$ inelastic collisions. This results in one EPS and $\bar{\nu}_h$ ETS, and therefore R_A in this approximation should be given by[13]

$$R_A \simeq \frac{1}{2} + \frac{\bar{\nu}_h}{2} , \qquad \text{(III.1)}$$

in agreement with feature (a) of Section II. The model also says that $(dN/d\eta)_{hA}$ should be approximately the same as $(dN/d\eta)_{hp}$ in the large η region,[14] and $(dN/d\eta)_{hA} \simeq \bar{\nu}_h (dN/d\eta)_{hp}$ in the small η region, in agreement with feature (b).

The above hh collision model is based on the recent discovery of the two-sheeted description of the Pomeron in the Dual Topological Unitarization (DTU) approach.[15] As we have just done, it can also be rephrased in the colored quark-parton model language.[16]

Even though we use the words projectile and target to describe the two excited hadronic systems, the quark-partons from which they are formed are not the same as those of the initial projectile and target.[12] Furthermore, unlike previously proposed two-fireball models[17] which were based on the fragmentation or diffractive model,[18] this DTU two-sheeted model is consistent with short-range correlation. In addition, at asymptotic energies, the two chains overlap completely in rapidity except for two finite regions at the two ends.

There is a small probability that the ETS's also do not evolve into their final states before reaching the succeeding nucleons and thereby undergo further interactions. This results in a second generation of ETS's and therefore additional multiplicity. Because of the low energy of the ETS's, the additional multiplicity should be small and in the small η region. The final hadrons from the evolution of the ETS's can also cascade, but this contribution can be neglected because the energies involved are even smaller. Therefore, this model predicts that R_A should be slightly larger than that given by (III.1), and the excess multiplicity should be in the small η region.

The above qualitative discussion has been made quantitative[12] by choosing a specific formulation of the two-sheeted hh model. The hh model chosen is that of Capella et al.[16a] This model was chosen because it is simple, well defined, and above all separates the contribution of the ETS from that of the EPS, but the results are fairly insensitive to the specific hh model used as input (as long as it agrees with the hh data).[19] The hA model is then completely determined and there is no free parameter. Figure 5a shows the results of these zero-parameter calculations for $dN/d\eta$ for 200 GeV p-initiated reactions for $\bar{\nu} = 2, 3, 4$, as well as the $\bar{\nu} = 1$ input. The model calculations are in good agreement with the data, except in the small η bins where as discussed before we expect the model calculations to underestimate the multiplicity. Similarly, good agreements are obtained at 100 GeV and 5C GeV, as shown in Figs. 5b and 5c. Figure 5d shows the model's prediction at 400 GeV.[20] The results for R_A are shown by the solid line in Fig. 6. Again, the model calculations are approximately equal to (but as expected slightly less than) the data.

As mentioned earlier, one expects an additional multiplicity for small η. Taking $\tau_0 \simeq \frac{1}{2m}$, one obtains the mean probability of an ETS reaching the next nucleon in A before evolving into its final state; then within the same two-sheeted model, it is straightforward combinatorials to trace its subsequent interactions with the succeeding nucleons (see Appendix B). The result for R_A after adding this additional contribution is the dashed line in Fig. 6. We see that the agreement is excellent.

Inasmuch as $\langle N_{ch} \rangle$ and $dN/d\eta$ for pN, πN, and kN are nearly the same, the model predicts that these quantities for pA, πA, and kA should be approximately the same for the same $\bar{\nu}$, in agreement with feature (c). In this model, because the energy of the EPS is only slightly smaller than the incident energy, the elasticity for pA is only slightly smaller than for pp, in agreement with feature (d).

Thus, we see that this simple two-sheeted model provides a good zero-parameter explanation of the first five experimental features. The only remaining feature to be explained (which has not yet been calculated in this model) is feature (f), the linear dependence of the dispersion D on $\langle N_{ch} \rangle$. Since it is known[21] for hh collisions that a two-component model can explain the dispersion data, by including a small diffractive component in the two-sheeted description of multiparticle production, one probably can explain this last feature also.

It is an interesting question whether the two methods of suppressing the degrees of freedom in the long-interaction-time model and the two-sheeted model are equivalent or different descriptions of the same physical phenomenon.

E. Other Models

We discuss a few other theoretical models. The parton model of Brodsky et al.[22] has similarity to the model of Ref. [10g]. The model assumes that on the average $\bar{\nu}_h$ wee-partons of the projectile interact with the wee-partons of the same rapidity in $\bar{\nu}_h$ different nucleons in A, and also assumes that cascading does not occur. It gives at asymptotic energy the result

$$R_A = \frac{\bar{\nu}_h}{\bar{\nu}_h + 1} + \frac{\bar{\nu}_h}{2} . \qquad \text{(III.2)}$$

In comparison with the two-chain model of Ref. [12], this parton model corresponds to a one-chain hh process. In addition, this model is applicable only in the central region, and the inclusion of the fragmentation contributions is done by the introduction of a parameter, whereas the model of Ref. [12] is valid for the whole rapidity range.

The two-phase model of Fishbane and Trefil[23] assumes that the first collision gives rise to an excited hadronic phase which has a flat distribution over the entire rapidity range and this excited phase has a long deexcitation time, and this excited hadronic phase interacts once more within A. However, the model neglects the interaction of the second (and subsequent) excited hadronic phase formed from the interaction of the first excited hadronic phase. Even ignoring this point, this model's dN/dy is different from that of Ref. [12] (even for the same hh input), because in the latter model the EPS while traversing A does not have much hadronic matter within the rapidity interval defined by its diquark and quark.

Finally we mention that there have been interesting attempts[24] in obtaining information from hA interactions about the number of constituent quark-partons in the incident hadrons.

IV. Nucleus-Nucleus Collisions

Some of the theoretical models discussed in the previous section can be easily generalized to nucleus-nucleus (AA) collisions. For illustration purposes, we discuss only the model of Ref. [12].[25] Analogous to the definition (II.1), one defines

$$\bar{\nu}_{A_1/A_2} \equiv \frac{A_1 \sigma_{in}^{NA_2}}{\sigma_{in}^{A_1A_2}} , \tag{IV.1}$$

which can be interpreted to be the average number of inelastically excited nucleons in A_1 in its collision with A_2. Then the two-sheeted model gives

$$R_{A_1A_2} \equiv \frac{\langle N_{ch}\rangle_{A_1A_2}}{\langle N_{ch}\rangle_{NN}} \simeq \frac{\bar{\nu}_{A_1/A_2}}{2} + \frac{\bar{\nu}_{A_2/A_1}}{2} , \tag{IV.2}$$

where the first (second) term is the contribution from the $\bar{\nu}_{A_1/A_2}$ ($\bar{\nu}_{A_2/A_1}$) excited projectile (target) systems in A_1 (A_2). Equation (IV.2) reduces to Eq. (III.1) when $A_1 = N$. The rapidity distribution $(dN/dy)_{A_1A_2}$ is given by superposing the contributions of $\bar{\nu}_{A_1/A_2}$ EPS's and $\bar{\nu}_{A_2/A_1}$ ETS's evaluated at the incident laboratory energy per nucleon. For the model to be realistic, the latter energy must be at least 20-30 GeV per nucleon. Unfortunately, this means that in the foreseeable future the only possible source of data is from cosmic rays.

V. Conclusion

The purpose of discussing high-energy hA collisions is to learn about the spacetime development of hh interactions and to differentiate various hh multiparticle production models. From the experimental data (especially features (a) and (b) presented in Section II and the theoretical analysis discussed in Section III), one concludes that to avoid excessive cascading there must be a long time scale involved in hh interactions. In the models of Ref. [10], this is the time it takes a high-energy hadron to generate a multiperipheral chain containing small rapidity partons so that it can have appreciable interaction with an at-rest hadron. Or saying it in another way, this is the time it takes a high-energy bare particle to dress up to be a physical hadron and so to have appreciable inelastic cross section upon collision with another hadron. In the model of Ref. [12], this is the time it takes the energetic excited projectile system to evolve into its final multihadron state. This long time scale rules out any sort of instantaneous production model such as the naive cascade model.

Some of the successful hA models also tie in with recent developments for models of hh interaction. For example, the models of Refs. [10f], [10g] and [22] rely heavily on parton model ideas, and the model of Ref. [12] is based on the two-sheeted description of the Pomeron and soft multiparticle production within the Dual Topological Unitarization approach.

As discussed in Section III, the latter model can also be rephrased using the language of colored quark-parton model and color confinement. All of this leads one to speculate that one can also see glimpses of the true underlying theory governing strong interaction by looking at hA interaction.

We also remark that there may be other interesting effects, besides the ones discussed here, which arise from interactions involving nuclear targets. One is the A-dependence for the inclusive cross section for large p_T secondaries. The data[26] shows that this A-dependence for a π secondary can be parametrized as $A^{\alpha(P_T)}$, where $\alpha(P_T) \approx 0.9$ for $P_T \lesssim 1$ GeV/c and increases to $\alpha(P_T) \approx 1.1$ for $P_T \gtrsim 4$ GeV/c. This A-dependence is most likely due to multiple scattering[27] inside the nucleus. Another effect is the apparently large intrinsic P_T that data involving nuclear targets seem to require for perturbative QCD to explain massive lepton pair production.[28] Perhaps at least part of this large intrinsic P_T is due to an increase in the effective intrinsic P_T as a result of multiple scattering inside the nucleus. Another effect is the importance of the two-step process $p + A \to \pi + A' + \cdots \to \mu^+\mu^- + \cdots$ as compared to the one-step process $p + A \to \mu^+\mu^- + \cdots$. Since the π has a valence antiquark, the two-step process may be significant if the production process is dominated by the Drell-Yan mechanism.[29]

We see that great progress in the field of hA interactions, both experimental and theoretical, was made during the last decade; we can look forward to some more exciting progress during this decade.

Acknowledgments

I wish to thank Professor Charles B. Chiu for collaboration and for valuable discussion, and for reading the manuscript and for useful suggestions. I also want to thank the Academia Sinica for the invitation to attend this Conference. This work was supported in part by the U.S. Department of Energy.

Appendix A

Here we present a simple argument within the disk approximation that $\bar{\nu}_h$ can be interpreted to be the average number of inelastic collisions experienced by h as it traverses A. Within this approximation one can relate[30] σ_{in}^{hN} and σ_{in}^{hA} to the S-matrix and get

$$\bar{\nu}_h = \frac{A\pi r_N^2(1 - S_h^2)}{\pi r_A^2(1 - S_h^{2\bar{k}})} , \qquad (A.1)$$

where $\bar{k}$ is the average (over impact parameter) number of nucleons in A lying along the path of h, r_N and r_A are the radii of a nucleon and the nucleus, respectively. But $\bar{k} \simeq A(r_N/r_A)^2$ and $S_h^{2\bar{k}} << 1$, so

$$\bar{\nu}_h \simeq \bar{k}(1 - S_h^2)$$

$$= \bar{k}P_h , \qquad (A.2)$$

where P_h is the inelastic collision probability.[10h] Our desired interpretation of $\bar{\nu}_h$ follows from Eq. (A.2).

For a more refined derivation, compare the theoretically calculated values of the average number of inelastic collisions obtained by Fishbane and Trefil[17b] and the experimental values of $\bar{\nu}_h$ of Ref. [3b].

Appendix B

In this appendix we consider pA collision and calculate the additional multiplicity due to the probability Q that the ETS does not evolve into its final multihadron state before reaching the succeeding nucleon N and thereby undergoes further interactions. We parametrize this probability by $e^{-t/\gamma\tau_0} \simeq e^{-2/\gamma}$, where we set $\tau_0 \simeq 1/2m_\pi$, and $t \simeq 1/m_\pi$ to be the time to travel the average internucleon distance, and γ is the time dilation factor.[31] Now, let P be the probability that an EPS or ETS would undergo an inelastic collision in a collision with N.[32] Then the probability P' that an EPS and ETS does not evolve into its final state after traveling the average internucleon distance and then undergoes an inelastic collision with the subsequent N is given by $P'_{EPS} \simeq P$ and $P'_{ETS} \simeq Pe^{-2/\gamma_{ETS}}$.

It suffices to include only those interactions of the ETS's with those succeeding N's which had not interacted inelastically with the EPS (we call these unwounded nucleons), because the excitation of N amounts to the formation of a sheet and this provides a natural saturation mechanism for its excitation.[33] We want to derive a formula for the average number $n_{\bar{k}}$ of inelastic collisions with unwounded nucleons that the ETS's experience in a nucleus with $\bar{k}$ nucleons ($\bar{k}$ is related to $\bar{\nu}_p$ by Eq. (A.2)). For $\bar{k} = 2$, n_2 is given by

Erratum

"What Can We Learn from High Energy Hadron-Nucleus Interactions?" by Don M. Tow, Univ. of Texas preprint ORO 3992-383 (Dec. 1979).

In Appendix B starting with the last two sentences on page 22, replace by the following:

... We want to derive a formula for the probability p_i that the unwounded ith nucleon experiences an inelastic collision with the preceding ETS's. It is obvious that p_2 is given by

$$p_2 \simeq P(1-P)P'_{ETS} , \tag{B.1}$$

where the first factor is the probability that the incident proton undergoes an inelastic collision with the first N to produce an ETS, the second factor is the probability that the EPS leaves the second N unwounded, and the third factor is the probability that the ETS does not evolve into its multihadron final state and then undergoes an inelastic collision with the second N. Similarly, p_3 is given by

$$p_3 \simeq [2P(1-P)](1-P)P'_{ETS} + P^2(1-P)[1 - (1 - P'_{ETS})^2] , \tag{B.2}$$

where the first (second) term is the contribution when there is one (two) ETS. The general formula is then

$$p_m \simeq \sum_{i=1}^{m-1} \phi_i^{m-1}(1-P)[1 - (1-P'_{ETS})^i] , \tag{B.3}$$

where

$$\phi_i^{\ell} = \frac{\ell!}{i!(\ell-i)!} P^i(1-P)^{\ell-i} . \tag{B.4}$$

The multiplicity from each such collision is to be evaluated at the laboratory energy of the ETS.[34] Also, only one-half of this is an additional multiplicity (as the contribution from the first generation ETS's is already included). The ratio r of this charged multiplicity to $\langle N_{ch}\rangle_{pN}$ (the latter evaluated at the incident energy) is approximately $r \simeq 0.27$.[35] Therefore, the additional contribution ΔR_A to R_A for a nucleus of $\bar{k}$ nucleons in length ($\bar{k}$ is related to $\bar{\nu}_p$ by Eq. (A.2)) is

$$\Delta R_A \simeq r \sum_{i=2}^{\bar{k}} p_i . \tag{B.5}$$

The quantitative results presented in the preprint are correct as they were calculated using the correct formulas as presented here.

$$n_2 \quad P(1-P)P'_{ETS} , \qquad \text{(B.1)}$$

where the first factor is the probability that the incident proton undergoes an inelastic collision with the first N to produce an ETS, the second factor is the probability that the EPS leaves the second N unwounded, and the third factor is the probability that the ETS does not evolve into its multihadron final state and then undergoes an inelastic collision with the second N. Similarly, for $\bar{k} = 3$, n_3 is given by

$$n_3 \simeq [2P(1-P)](1-P)P'_{ETS} + P^2(1-P)[1 - (1 - P'_{ETS})^2] , \qquad \text{(B.2)}$$

where the first (second) term is the contribution when there is one (two) ETS. The general formula is then

$$n_{\bar{k}} \simeq \sum_{i=1}^{\bar{k}-1} \phi_i^{\bar{k}-1} (1-P)[1 - (1-P'_{ETS})^i] , \qquad \text{(B.3)}$$

where

$$\phi_i^{\ell} = \frac{\ell!}{i!(\ell-i)!} P^i (1-P)^{\ell-i} . \qquad \text{(B.4)}$$

The multiplicity from each such collision is to be evaluated at the laboratory energy of the ETS.[34] Also, only one-half of this is an additional multiplicity (as the contribution from the first generation ETS's is already included). The ratio r of this charged multiplicity to $\langle N_{ch}\rangle_{pN}$ (the latter evaluated at the incident energy) is approximately $r \approx 0.27$.[35] Therefore, to find the additional contribution to R_A, one just multiplies $n_{\bar{k}}$ given by Eq. (B.3) by this r.

References and Footnotes

[1] Macroscopic distance here means any distance which is much larger than the typical range of strong interaction, i.e., 1 Fermi.

[2] For previous reviews, see

a. K. Gottfried, in Proc. of the V Intern. Conf. on High Energy Physics and Nuclear Structure-1973, Uppsala, Sweden, ed. by G. Tibell (North-Holland, Amsterdam/American Elsevier, New York, 1974).

b. W. Busza, in Proc. of the VI Intern. Conf. on High Energy Physics and Nuclear Structure-1975, Santa Fe and Los Alamos, U.S.A., ed. by D. E. Nagle et al. (American Institute of Physics Conf. Proc. No. 26, New York, 1975).

c. L. Bertocchi, ibid.

d. N. N. Nikolaev, in Proc. of the Trieste Topical Meeting on the Multiple Production on Nuclei-1976, ed. by L. Bertocchi.

e. A. Bialas, talk presented at the First Workshop on Ultra-Relativistic Nuclear Collisions, Berkeley, 1979; Fermilab preprint FERMILAB-Conf-79/35-THY (1979).

[3] a. W. Busza et al., Phys. Rev. Lett. 34, 836 (1975).

b. W. Busza et al., in Proc. of the XVIII Intern. Conf. on High Energy Physics, Tbilisi, 1976, ed. by N. N. Bogoliubov et al. (JINR, Dubna, U.S.S.R., 1977).

c. J. R. Florian et al., Phys. Rev. D13, 558 (1976).

d. C. Halliwell et al., Phys. Rev. Lett. 39, 1499 (1977).

e. D. Chaney et al., ibid. 40, 71 (1978).

f. J. E. Elias et al., ibid. 41, 285 (1978).

g. D. Chaney et al., Phys. Rev. D19, 3210 (1979).

h. J. E. Elias et al., Fermilab preprint FERMILAB-PUB-79/47-EXP 7185.178 (1979).

[4] The constant b (a) is slightly larger (smaller) than 1/2.

[5] See, e.g., Ref. [3g].

[6] a. P. M. Fishbane and J. S. Trefil, Phys. Rev. D3, 231 (1971).

b. A. Dar and J. Vary, ibid. D6, 2412 (1972).

[7] By physical or fully dressed secondary we mean that it has the same inelastic collision probability as an ordinary hadron.

[8] a. A. Z. Patashinskii, Zh. Eskp. Teor. Fiz. Pis'ma Red. 19, 654 (1974) [JETP Lett. 19, 338 (1974)].

b. F. Takagi, Nuovo Cimento Lett. 14, 559 (1975).

c. G. Berlad, A. Dar and G. Eilam, Phys. Rev. D13, 161 (1976).

d. S. Fredricksson, Nucl. Phys. B111, 167 (1976).

e. Meng Ta-Chung, Phys. Rev. D15, 197 (1977).

[9] A. M. Baldin et al., Yad. Fiz. 20, 1201 (1974) [Engl. Trans. 20, 629 (1975)]. See also A. M. Baldin, in Proc. of the VI Intern. Conf. on High Energy Physics and Nuclear Structure-1975, ibid.

[10] a. E. L. Feinberg, Zh. Eksp. Teor. Fix. 50, 202 (1966) [Sov. Phys.-JETP 23, 132 (1966)].

b. O. V. Kancheli, Zh. Eksp. Teor. Fiz. Pis'ma Red. 18, 465 (1973) [JETP Lett. 18, 274 (1974)].

c. E. S. Lehman and G. A. Winbow, Phys. Rev. D10, 2962 (1974).

d. J. Koplik and A. H. Mueller, Phys. Rev. D12, 3638 (1975).

e. L. Stodolsky, in Proc. of the VI Symp. on Multiparticle Dynamics, Oxford, 1975.

f. G. V. Davidenko and N. N. Nikolaev. Yad. Fiz. 24, 772 (1976) [Engl. Trans. 20, 402 (1976)].

g. A. Capella and A. Kryzwicki, Phys. Lett. 67B, 84 (1977), Phys. Rev. D18, 3357 (1978).

h. G. Bialkowski, C. B. Chiu, and D. M. Tow, Phys. Lett. 68B, 451 (1977), Phys. Rev. D17, 862 (1978). M. Hossain and D. M. Tow, Phys. Rev. D (to be published).

i. P. Valanju, E.C.G. Sudarshan, and C. B. Chiu, Phys. Rev. D (to be published).

[11] See the third paper of Ref. [10h].

[12] Chao W.-q., C. B. Chiu, He Z., and D. M. Tow, University of Texas preprint ORO 3992-376 (1979).

[13] Energy momentum conservation correction to this result can be shown[12] to be small.

[14] Since the EPS has a slightly smaller energy than its parent, $(dN/d\eta)_{hA}$ is actually slightly smaller than

$(dN/d\eta)_{hp}$ for $\eta \sim \eta_{max}$, in agreement with feature (e).

[15] a. H. Lee, Phys. Rev. Lett. 30, 719 (1973).

b. G. Veneziano, Phys. Lett. 43B, 413 (1973), 52B, 220 (1974), Nucl. Phys. B74, 365 (1974).

c. H.-M. Chan, J. E. Paton, and S. T. Tsou, Nucl. Phys. B86, 479 (1975); H.-M. Chan, J. E. Paton, S. T. Tsou, and S. W. Ng, Nucl. Phys. B92, 13 (1975).

d. For a review, see, e.g., G. F. Chew and C. Rosenzweig, Phys. Rep. 41C, 263 (1978).

e. For a discussion of the similarity between the DTU Pomeron and the dual resonance model Pomeron, see C. B. Chiu and S. Matsuda, Nucl. Phys. B134, 463 (1978), P. Aurenche and L. Gonzalez-Mestres, Phys. Rev. D18, 2995 (1978).

[16] a. A. Capella, U. Sukhatme, C.-I Tan, and J. Tran Thanh Van, Phys. Lett. 81B, 68 (1979).

b. A. Capella, U. Sukhatme, and J. Tran Thanh Van, Orsay preprint LPTPE 79/23 (1979). This is a refinement of the model of Ref. [16a]. It also eliminates an objection recently raised by W. Ochs and T. Shimada, Max-Planck Institute preprint MPE-PAE/PTh 34/79 (1979).

c. G. Cohen-Tannoudji et al., Saclay preprint DPh-T/79-97 (1979), and references therein.

d. For similar ideas, see also J. Dias de Deus and S. Jadach, Acta Phys. Polon. B9, 249 (1978).

[17] a. A. Dar and J. Vary, Phys. Rev. D6, 2412 (1972).

b. P. M. Fishbane and J. S. Trefil, Phys. Rev. D9, 168 (1974).

[18] a. C. Quigg, J.-M. Wang, and C. N. Yang, Phys. Rev. Lett. 1290 (1972).

b. R. Hwa, ibid. 26, 1143 (1971).

c. M. Jacob and R. Slansky, Phys. Rev. D5, 1847 (1972).

[19] For example, using the more refined version of Ref. [16b] gives essentially the same conclusions.

[20] There is one set of experimental data at 400 GeV [F. Fumuro, R. Ihara, and T. Ogata, Nucl. Phys. B152, 376 (1979)]. However, their normalization seems to be very different from those at several lower energies (50-300 GeV).[3]

[21] a. L. Van Hove, Phys. Lett. 43B, 65 (1973).

b. K. Fialkowski and H. I. Miettinen, Phys. Lett. 43B, 493 (1973).

c. C. B. Chiu and K.-H. Wang, Phys. Rev. D8, 2929 (1973).

[22] S. J. Brodsky, J. F. Gunion, and J. H. Kühn, Phys. Rev. Lett. 39, 1120 (1977).

[23] P. M. Fishbane and J. S. Trefil, Phys. Lett. 51B, 139 (1974).

[24] a. A. Bialas, W. Czyz, W. Furmanski, Acta Phys. Polon. B8, 585 (1977).

b. V. V. Anisovich, Yu. M. Shabelsky, and V. M. Shekhter, Nucl. Phys. B133, 477 (1978).

c. N. N. Nikolaev and A. Ya. Ostapchuck, CERN preprint

Ref. TH. 2575-CERN (1978).

d. See also A. S. Goldhaber, Phys. Rev. Lett. 33, 47 (1974).

[25] See also the discussion in Ref. [22].

[26] a. J. W. Cronin et al., Phys. Rev. D11, 3105 (1975).

b. L. Kluberg et al., Phys. Rev. Lett. 38, 670 (1977).

[27] J. H. Kühn, Phys. Rev. D13, 2948 (1976).

[28] See, e.g., R. C. Hwa, in Proc. of the XIII Rencontre de Morioud, Les Arcs, France, ed. by J. Tran Thanh Van, 1978.

[29] S. D. Drell and T. M. Yan, Phys. Rev. Lett. 25, 316 (1970); Ann. Phys. (N.Y.) 66, 578 (1971).

[30] See the first two papers of Ref. [10h] and Footnote 10 of the third paper of this reference.

[31] For an incident energy of 200 GeV, within the model of Ref. [12], γ_{EPS} and γ_{ETS} are respectively 34 and 3. Therefore, this probability Q for the EPS can be set approximately equal to one.

[32] In the numerical calculation we assume that the EPS or ETS has the same P as that of a proton which was estimated in Ref. [10b] to be 0.64.

[33] Another argument to support this assertion is because two ETS's have small relative momentum and so even upon a collision very little additional multiplicity will result.

[34] Within the model of Ref. [12], this energy is ~17 GeV when the incident energy is 200 GeV.

[35] See, e.g., D. M. Tow, Phys. Rev. D7, 3535 (1973).

Figure Captions

1. The multiplicity ratio R_A versus $\bar{\nu}_p$ for 200 GeV pA collisions. Data is from Ref. [3b].
2. Laboratory pseudorapidity distributions $dN/d\eta$ for pA collisions. Data is from Ref. [3b].
3. The multiperipheral chain developments of a secondary with large rapidity y_ℓ and one with small rapidity y_s. The former does not interact with the nucleus whose nucleons are denoted by dots. The y-axis denotes rapidity.
4. The two-sheeted model for multiparticle production: (a) at short times, (b) at long times.
5. Laboratory pseudorapidity distributions $dN/d\eta$ for pA collisions. Solid curves are the zero-parameter results of the two-sheeted model of Ref. [12]; the $\bar{\nu} = 1$ curve is the input.
   (a) At 200 GeV. Also shown are the individual contributions (dashed curves) of the EPS and ETS. The histograms are the data of Ref. [3b].
   (b) At 100 GeV. The histograms are the data of Ref. [3h].
   (c) At 50 GeV. The histograms are the data of Ref. [3h].
   (d) Predictions at 400 GeV.
6. The multiplicity ratio R_A versus $\bar{\nu}_p$ for 200 GeV pA collisions. Data is from Ref. [3b]. The dashed line and solid line are the results of Ref. [12] with and without including further interactions of the ETS's as explained in the text.

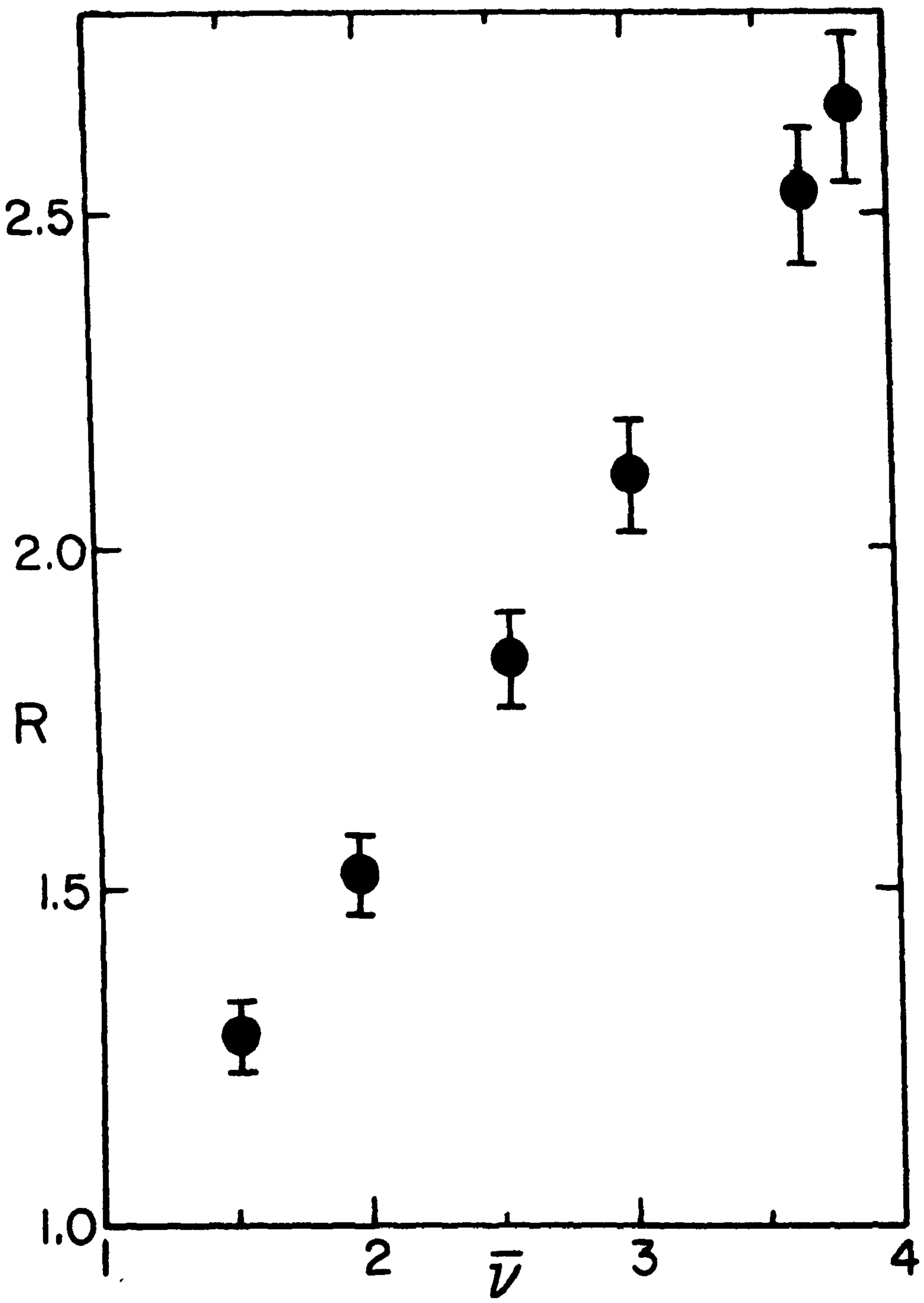

Fig. 1

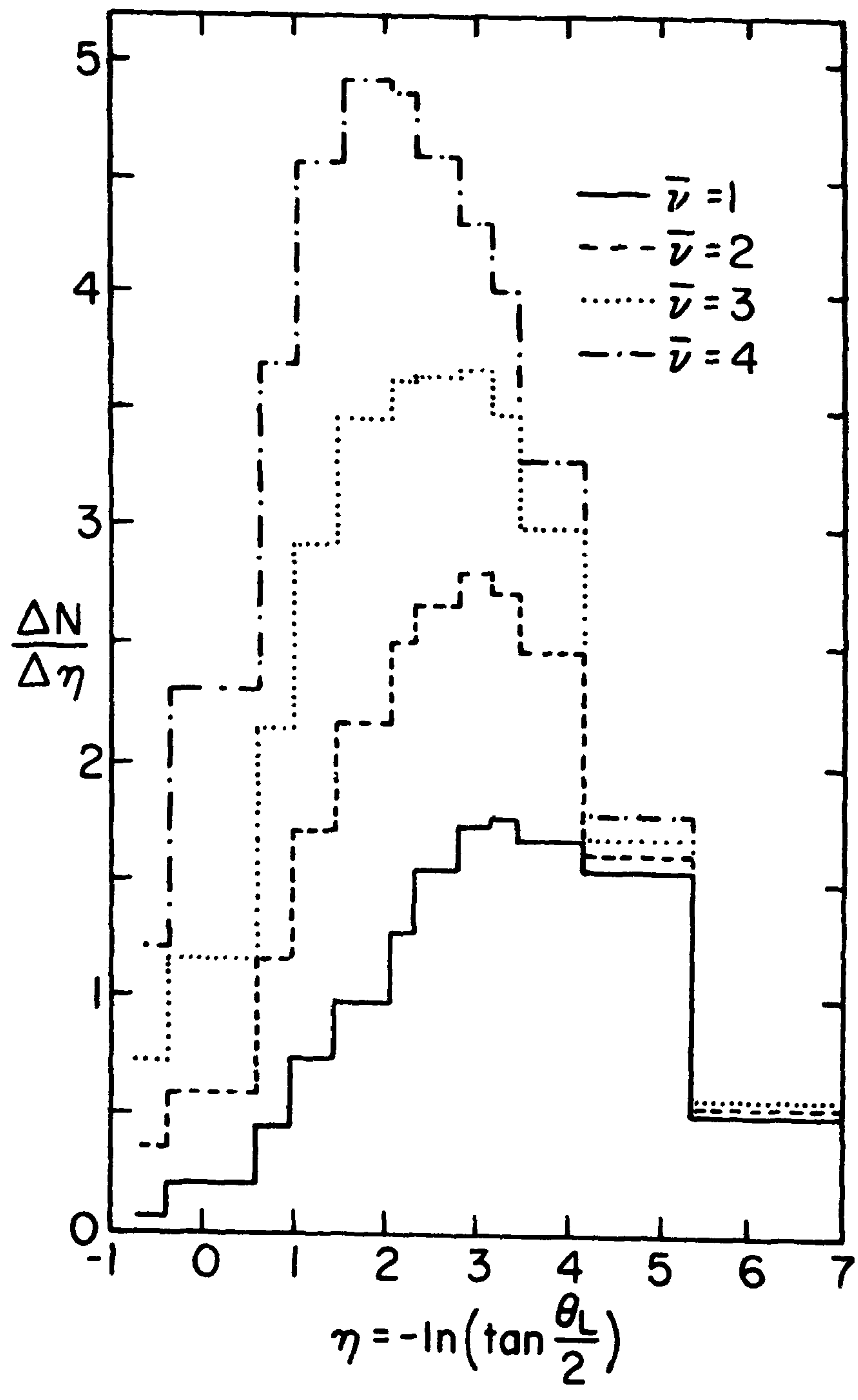
5
4
3
2
1
0
$\frac{\Delta N}{\Delta \eta}$
-1
0
1
2
3
4
5
6
7
$\eta = -\ln\left(\tan\frac{\theta_L}{2}\right)$
$\bar{\nu} = 1$
$\bar{\nu} = 2$
$\bar{\nu} = 3$
$\bar{\nu} = 4$

Fig. 2

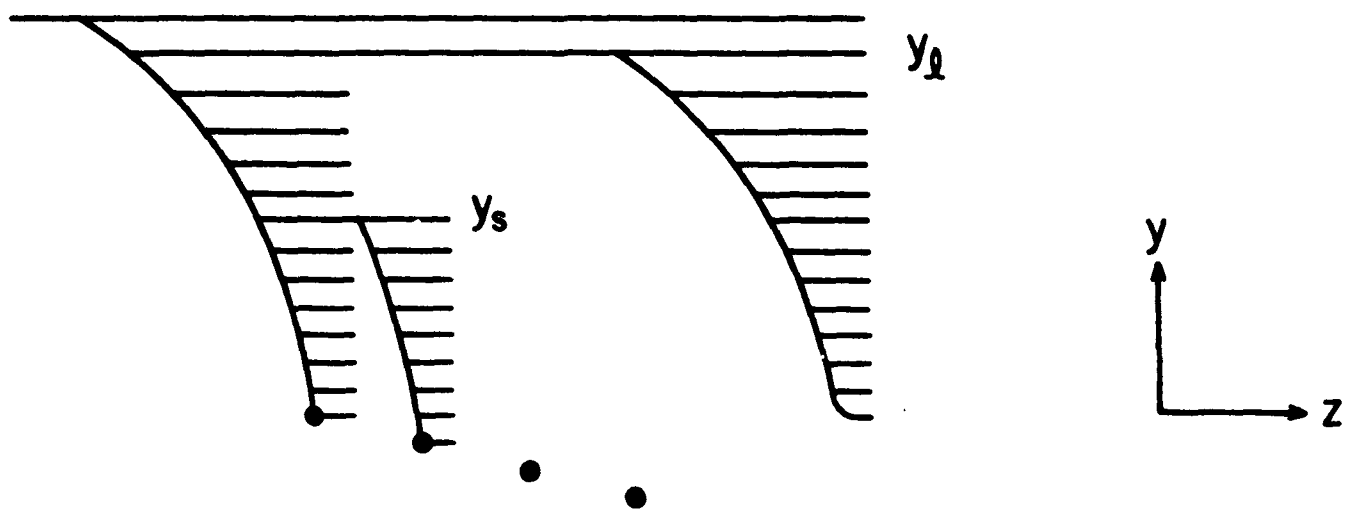

Fig. 3

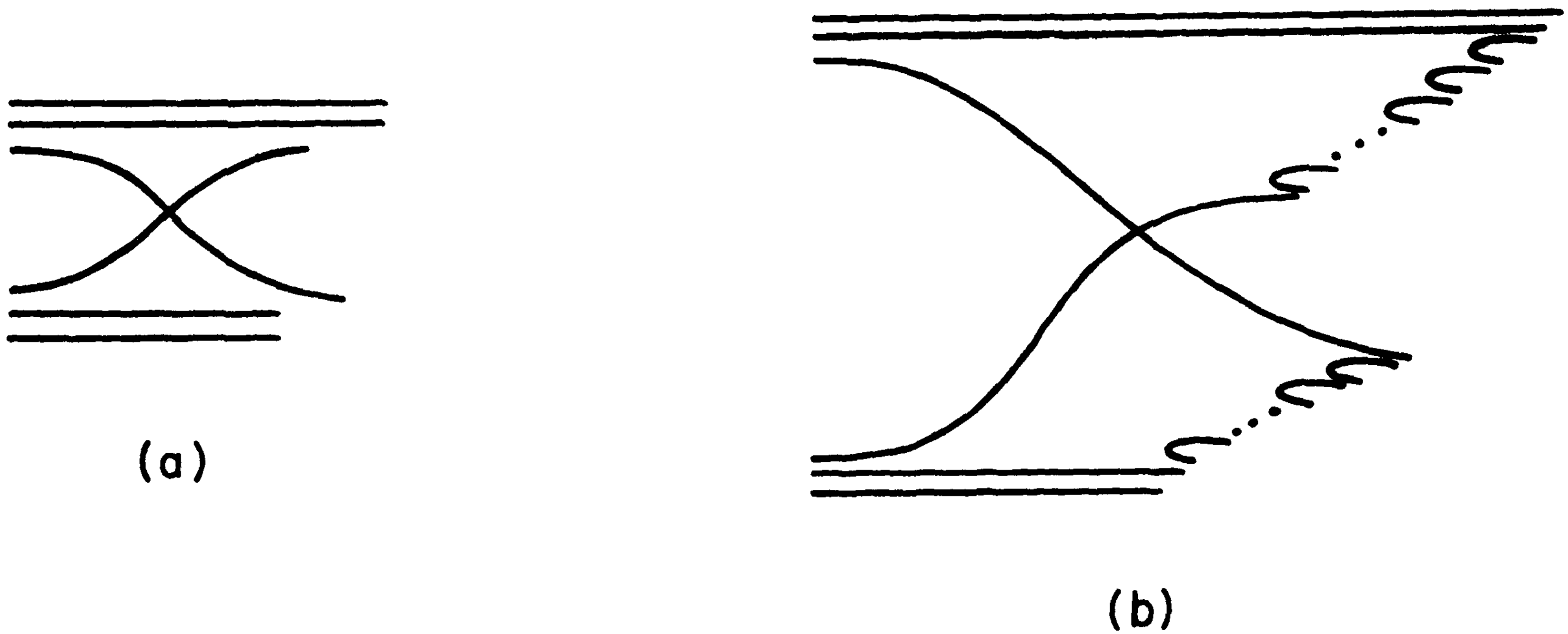

Fig. 4

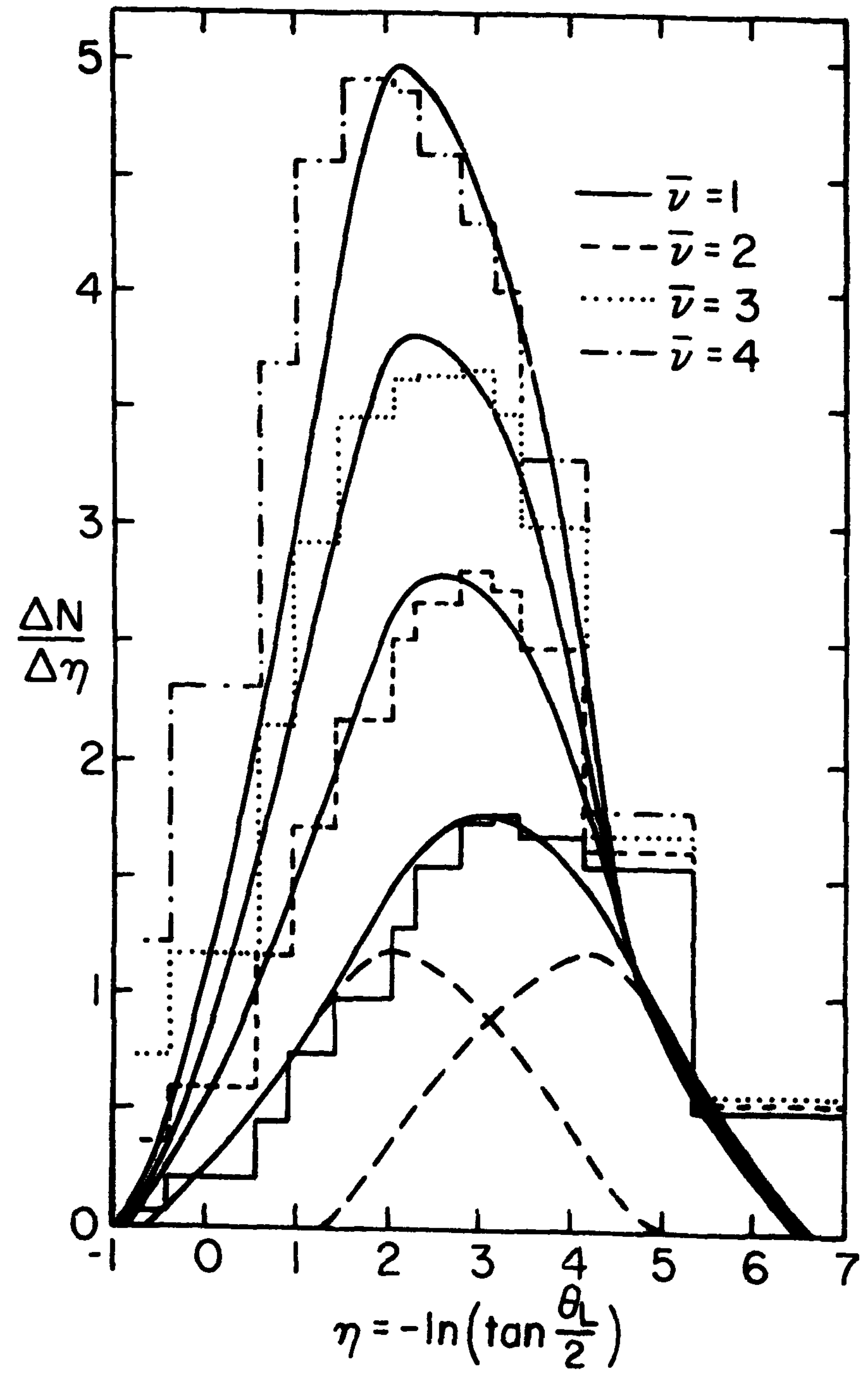

5
4
3
2
1
0
-1
0
1
2
3
4
5
6
7
$\frac{\Delta N}{\Delta \eta}$
$\eta = -\ln\left(\tan\frac{\theta_L}{2}\right)$
$\bar{\nu} = 1$
$\bar{\nu} = 2$
$\bar{\nu} = 3$
$\bar{\nu} = 4$

Fig. 5a

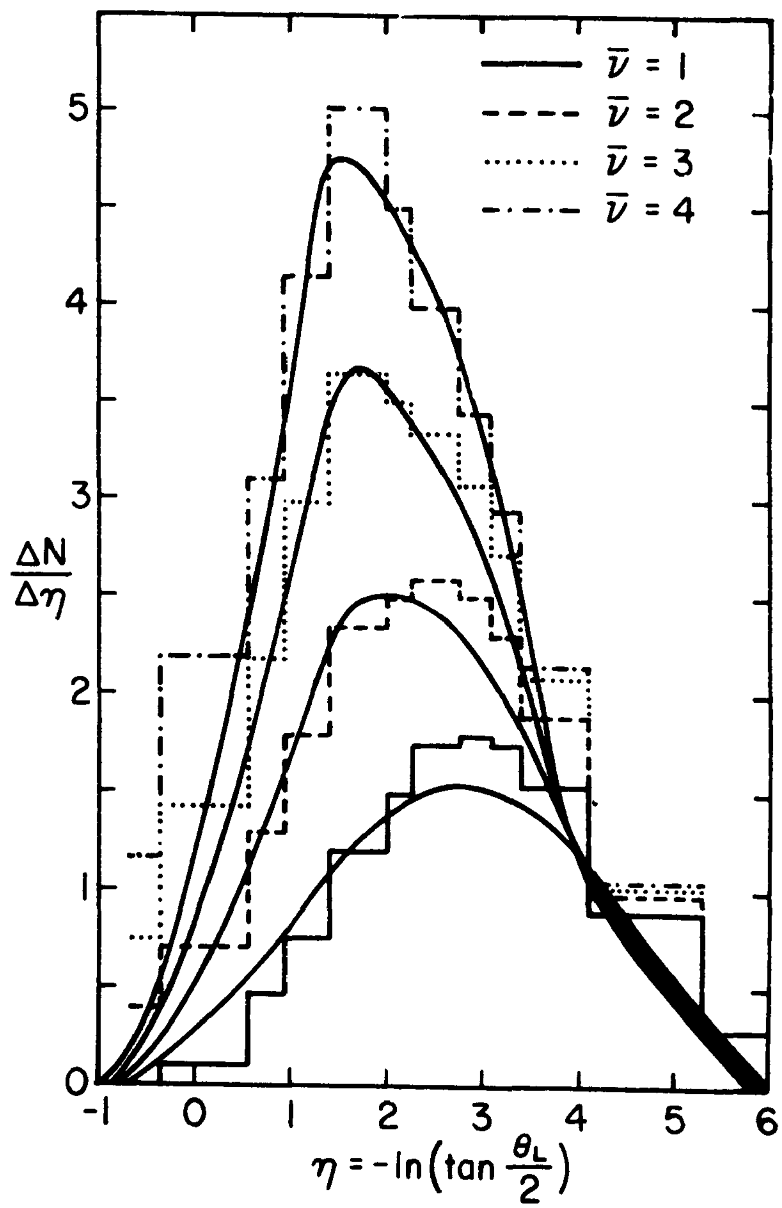
$\bar{\nu}$ = 1
$\bar{\nu}$ = 2
$\bar{\nu}$ = 3
$\bar{\nu}$ = 4
5
4
3
2
1
0
$\frac{\Delta N}{\Delta \eta}$
-1
0
1
2
3
4
5
6
$\eta = -\ln\left(\tan \frac{\theta_L}{2}\right)$

Fig. 5b

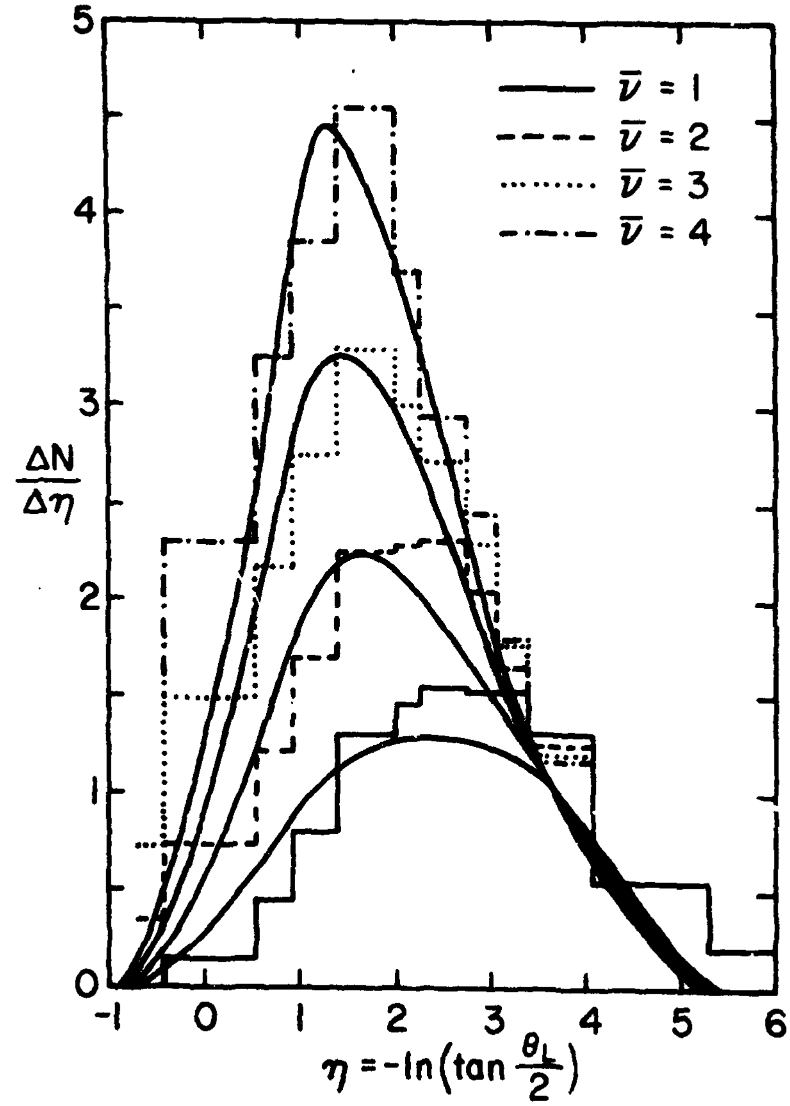

Fig. 5c

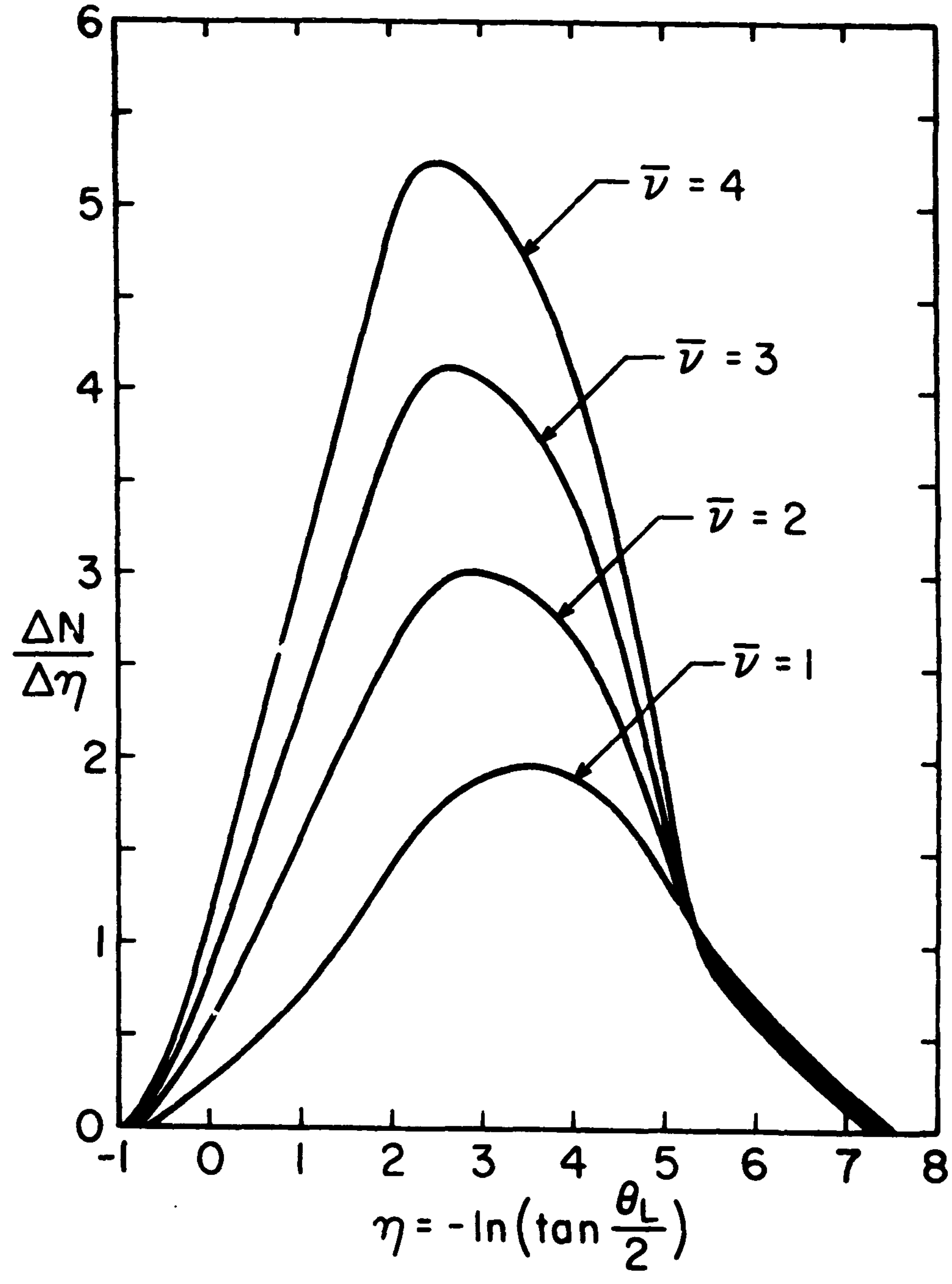
6
5
4
3
2
1
0
$\frac{\Delta N}{\Delta \eta}$
$\bar{\nu} = 4$
$\bar{\nu} = 3$
$\bar{\nu} = 2$
$\bar{\nu} = 1$
-1 0 1 2 3 4 5 6 7 8
$\eta = -\ln\left(\tan \frac{\theta_L}{2}\right)$

Fig. 5d

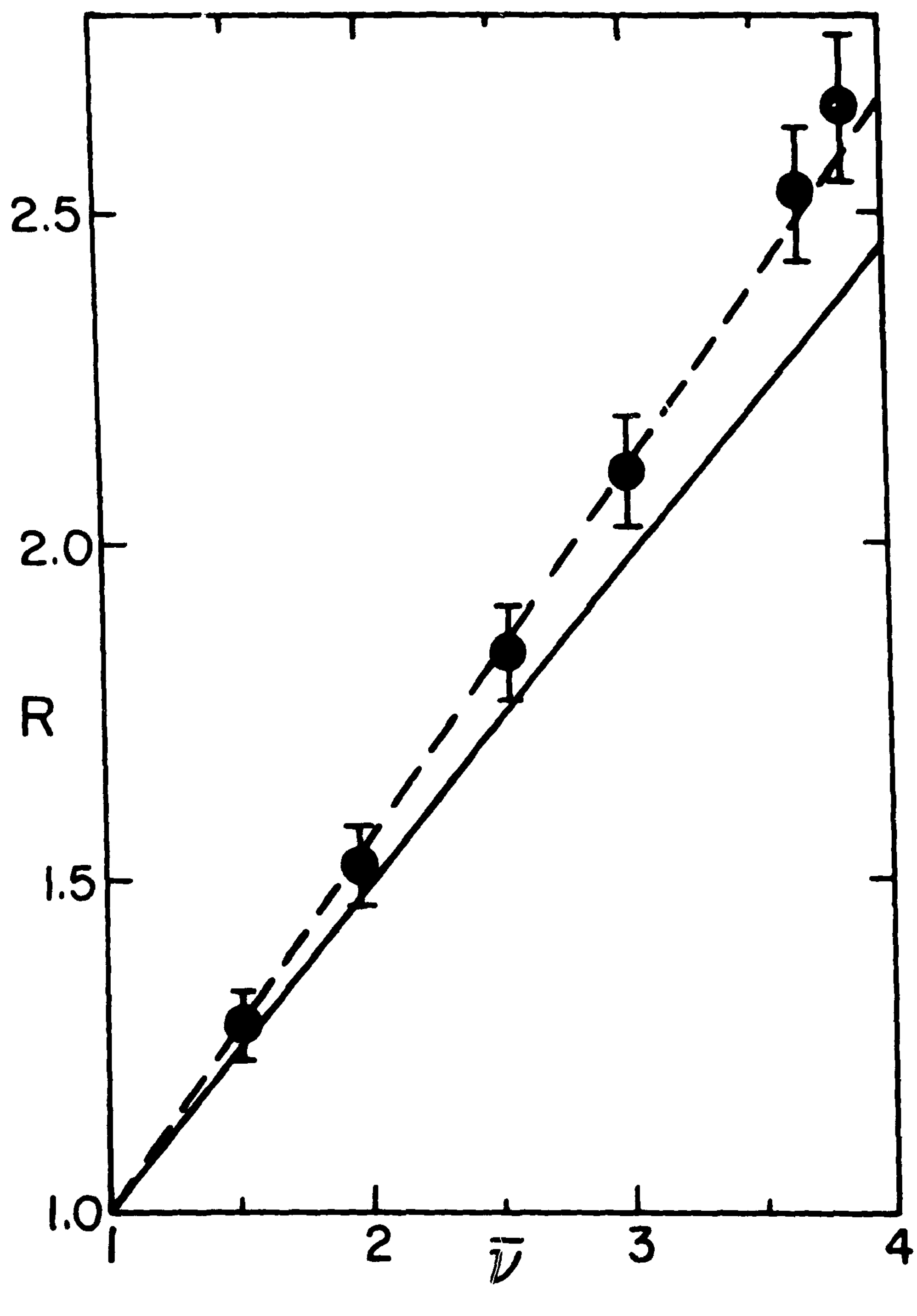

Fig. 6